THE BIREFRINGENCE OF WOOD PULP FIBRES AND THE THICKNESS OF THE S_1 AND S_3 LAYERS

D. H. Page and *F. El-Hosseiny*
Pulp and Paper Research Institute of Canada, Pointe-Claire, P. Q., Canada H9R 3J9

(Received 13 May 1974)

ABSTRACT

The birefringence of pulped softwood fibres has been measured and found for several species to decrease with decreasing cell-wall thickness. This is explained theoretically by the compensation of the retardation of light in the S_2 layer by the transversely wound S_1 and S_3 layers. These layers are of similar thickness for all fibres and thus have a greater effect on thin-walled fibres. Measurement of birefringence over a range of fibre wall thicknesses permits a determination of the thickness of the S_1 and S_3 layers, and the results are in good agreement with data from other methods.

Additional keywords: Fibres, cellulose fibres, softwoods, birefringence, optical properties, fibrils, angles, cell-wall thickness, fibre structure, microstructure, cell walls, primary walls, secondary walls.

INTRODUCTION

The structure of a softwood fibre is shown in Fig. 1 (Kerr and Bailey 1934). It consists of a tenuous primary wall, P, heavily encrusted with lignin to form the middle lamella, ML, and three secondary layers, S_1, S_2, and S_3, composed of cellulosic fibrils embedded in an amorphous matrix of hemicellulose and lignin. The S_1 and S_3 layers are thin and the fibrils are wound almost transversely to the fibre axis. The S_2 layer comprises most of the cell wall and its fibrils are wound in a helix at an angle, termed the fibril angle, to the fibre axis. The fibrils are largely crystalline and are aligned in the secondary layers so that wood fibres are in general birefringent. The magnitude of the birefringence depends on the relative thicknesses of the layers, ML-P, S_1, S_2, and S_3, and the orientation and birefringence of each layer. A theoretical equation has been derived for the birefringence of wood fibres of low fibril angle and verified experimentally. From birefringence measurements a precise measure of the average combined thickness of the S_1 and S_3 layers can be derived.

THEORY

We will consider a wood pulp fibre viewed between crossed polars in a microscope, the axis of which is perpendicular to the fibre axis. The fibrils of S_2 make an angle θ with the fibre axis. The S_1 layer is generally considered to comprise several layers of fibril angle 70–80° with alternating S and Z helices. The optical behaviour of such a structure is approximately equivalent to a single layer of fibril angle 90°. For the analysis given here, the fibrils of S_1 are thus assumed to be perpendicular to the fibre axis. The S_3 layer is treated similarly. Plane polarized light entering a birefringent layer of the fibre is split into ordinary and extraordinary components that travel at different velocities. These components are subsequently split again as they pass each layer boundary. The complete theory of the state of the emergent light is complicated. Generally, it belongs to the theory of "elliptical retarders" and the term "birefringence" is not used for such structures. The problem simplifies if we consider only fibres for which the fibril angle of the S_2 layer is zero. Then polarized light is split into two components on entering the fibre, vibrating in the directions parallel and perpendicular to the fibre axis, but is not split again as it passes through the various layers. Such a fibre is a linear retarder and the term "birefringence" is defined as the difference between the refractive indices for light

beams vibrating parallel and perpendicular to the fibre axis.

Since the S_1 and S_3 layers have their directions of maximum refractive index perpendicular to that of the S_2 layer, they in part compensate for the retardation in the S_2 layer.

The retardation R of the fibre thus becomes

$$R = 2(\mu_2 t_{S_2} - \mu_1 t_{S_1} - \mu_3 t_{S_3}) \quad (1)$$

where μ_1, μ_2, μ_3, are the birefringences and t_{S_1}, t_{S_2}, t_{S_3} are the thicknesses of the S_1, S_2, and S_3 layers, respectively. We assume that the middle lamella is unoriented and its birefringence is zero.

The light path 2T is given by

$$2T = 2\left(t_{S_1} + t_{S_2} + t_{S_3} + t_{ML+P}\right) \quad (2)$$

where T is the total thickness of a single cell wall.

Birefringence of the fibre μ_f is then given by

$$\mu_f = \frac{R}{2T} = \frac{\mu_2 t_{S_2} - \mu_1 t_{S_1} - \mu_3 t_{S_3}}{t_{S_1} + t_{S_2} + t_{S_3} + t_{ML+P}} . \quad (3)$$

We wish now to consider fibres pulped by a process of complete delignification. The middle lamella, being composed mostly of lignin, is dissolved during pulping and can be ignored. We will assume that the chemical composition and degree of molecular orientation of the pulped S_1, S_2, and S_3 layers are similar, so that

$$\mu_1 = \mu_2 = \mu_3 = \mu_0 . \quad (4)$$

Then

$$\mu_f = \mu_0 \left\{1 - 2 \frac{\left(t_{S_1} + t_{S_3}\right)}{T}\right\} \quad (5)$$

Insofar as the assumption of the constancy of chemical composition between the layers is invalid, the thicknesses t_{S_1} and t_{S_3} can be regarded as equivalent rather than absolute thicknesses.

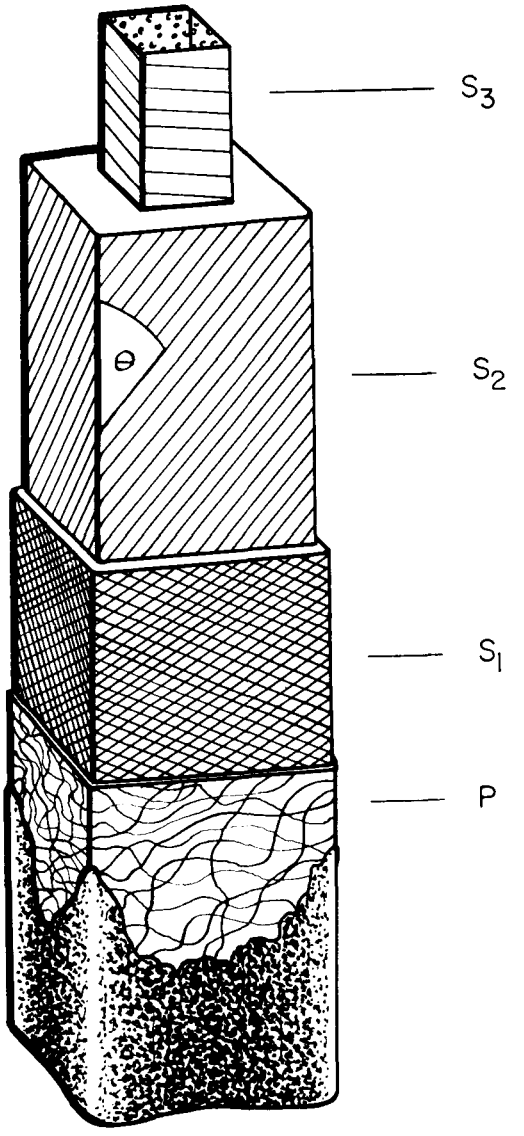

FIG. 1. Schematic representation of a single fibre of wood showing the arrangement of the cellulosic microfibrils in the various layers of the cell wall.

The theory given above is only strictly correct for fibres of zero fibril angle. We have applied the theoretical equation of Hsu et al. (1947) to the general case when the fibril angle is not zero and have verified that no serious error arises provided the fibril angle is smaller than 10°. Our experimental verification was carried out on fibres of fibril angle between 0° and 10°.

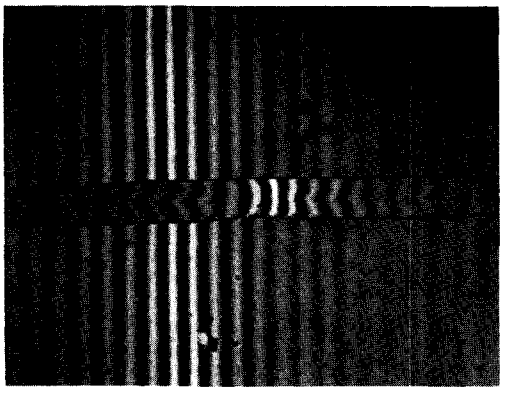

FIG. 2. Interference micrograph taken in fringe field conditions for measurement of wall thickness at a specified location on the fibre.

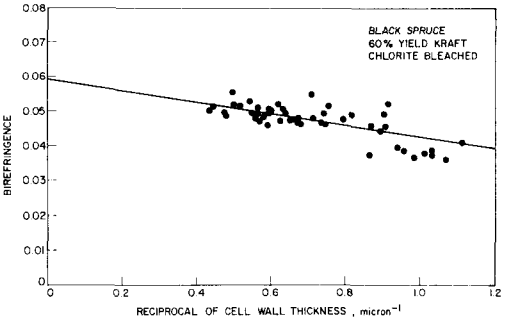

FIG. 3. Plot of birefringence against reciprocal of cell-wall thickness for black spruce fibres, 60% yield kraft, chlorite bleached.

The theory predicts that the birefringence of fibres will be a function of the thickness, T, of the cell wall. The nature of the function depends on the relationship between t_{S_1}, t_{S_3}, and T. We will consider three cases.

I. *The thicknesses of S_1 and S_3 are a constant proportion of the total thickness T.*

$$t_{S_1} + t_{S_3} = K_1 T \qquad (6)$$

Hence,

$$\mu_f = \mu_0 (1 - 2 K_1) \quad . \qquad (7)$$

In this case the birefringence of all fibres is the same, but is lower than the birefringence of cell-wall material μ_0, by a factor that depends on the ratio of the thicknesses of the layers.

II. *The S_1 and S_3 layers are of constant thickness and the variation in the total thickness T, from fibre to fibre, comes from variation in the S_2 layer.*

$$t_{S_1} = K_2, \quad t_{S_3} = K_3 \qquad (8)$$

Hence,

$$\mu_f = \mu_0 \left[1 - 2 \frac{(K_2 + K_3)}{T}\right] \quad . \qquad (9)$$

In this case the birefringence varies with T, the thickest fibres having a birefringence that approaches that of cell-wall material.

III. *The S_1 and S_3 thicknesses are partly constant and partly variable with T.*

$$t_{S_1} + t_{S_3} = K_4 + K_5 T \qquad (10)$$

Hence,

$$\mu_f = \mu_0 \left[1 - 2 K_5 - \frac{2K_4}{T}\right] \quad . \qquad (11)$$

Here, the birefringence of the fibre varies with T as in case II, but even for the thickest fibres the birefringence does not approach that of the cell-wall material.

The relevance of the three cases will be apparent in the analysis of the data.

EXPERIMENTAL

Wood pulp fibres of several softwood species were pulped as indicated in Table 1. The pulps were dried in the form of loose filtered mats and impregnated with mercury for the determination of fibril angle. The pulps were resuspended and fibres were dried individually between a cover glass and microscope slide. The fibril angle of each fibre was determined, by the method of Page (1969), and only those fibres with fibril angle less than 10° were accepted.

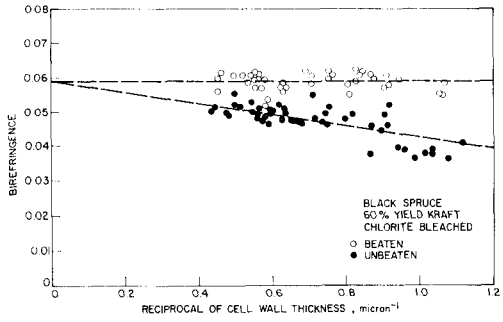

FIG. 4. Plot of birefringence against reciprocal of cell-wall thickness for unbeaten and beaten black spruce fibres, 60% yield kraft, chlorite bleached. The regression lines have a common intercept.

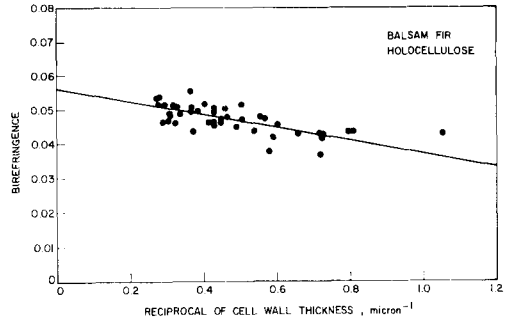

FIG. 6. Plot of birefringence against reciprocal of cell-wall thickness for balsam fir holocellulose.

Birefringence was determined from two measurements, thickness, T, and retardation in polarized light, R. The dry fibres were first observed in a Leitz interference microscope in fringe field conditions using transmitted light. The shift in the fringes caused by the light passing through the fibre was measured by using a compensating calibrated wedge, adjusted to bring the fringes in the fibre to the same position as the fringes in the background. This measurement gives the value $(n - 1)2T$ where n is the mean refractive index of the fibre and 2T is the length of the light path through the fibre. T was calculated assuming a value of 1.570 for n. The maximum error in T arising from this assumption was estimated at 2%. A Polaroid photograph was taken of every fibre to record the exact location of the point of measurement, which was generally at a point in the fibre axis in a region where the lumen did not contain mercury droplets. A typical print is shown in Fig. 2.

The slide was then transferred to a polarizing microscope and the region of measurement located. The retardation in transmitted polarized light, R, was determined by orienting the fibre at 45° to the crossed polars and using a calibrated Ehringhaus compensator to achieve extinction. The birefringence is given by

$$\mu_f = n_{\parallel} - n_{\perp} = \frac{R}{2T} . \qquad (12)$$

The experimental error in birefringence and 2T was determined from separate measurements by two operators on the same fibre. The mean error in birefringence was 0.001 and in 2T, 0.07μm.

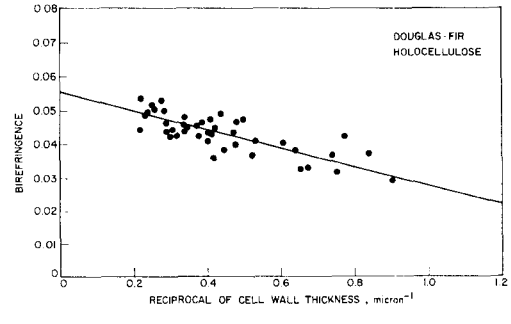

FIG. 5. Plot of birefringence against reciprocal of cell-wall thickness for Douglas-fir holocellulose.

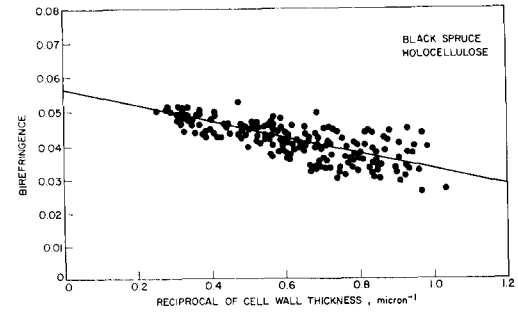

FIG. 7. Plot of birefringence against reciprocal of cell-wall thickness, for black spruce holocellulose.

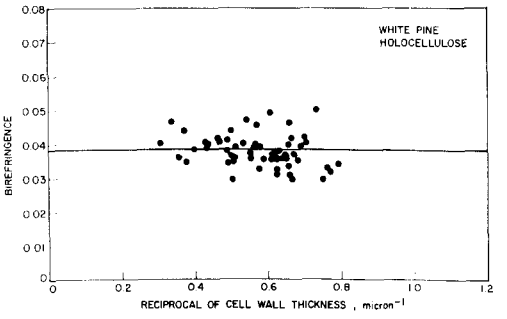

FIG. 8. Plot of birefringence against reciprocal of cell-wall thickness for white pine holocellulose.

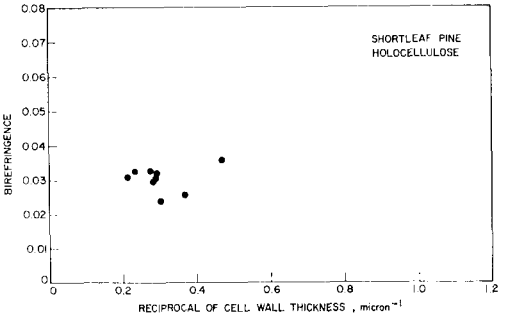

FIG. 9. Plot of birefringence against reciprocal of cell-wall thickness for shortleaf pine holocellulose.

RESULTS AND DISCUSSION

The theory for cases II and III predicts a linear relationship between birefringence and the reciprocal of the wall thickness. All the data are therefore plotted in this way in Figs. 3 to 10. Since R and T are the measured variables, regression lines were obtained of the form $R = a_0 + a_1T$, and were subsequently transposed to the form $\mu_f = b_0 + b_1/T$, for presentation on the graphs.

Black spruce kraft pulp, chlorite bleached

For this pulp, the data fall on a line of negative slope, supporting the theory, as shown in Fig. 3. The distinction is not clear, however, between case II, in which the thickness of the S_1 and S_3 layers are constant and case III, in which the thicknesses are partly constant and partly variable. Neither is it certain that the birefringence is being controlled according to the theory, and not by a fortuitous relationship between the cell-wall thickness and the degree of orientation of cellulose in the cell wall. For this species, the S_3 layer is of negligible thickness. The matter can therefore be decided by beating the pulp until the S_1 layer is removed. According to case II, the birefringence should then be independent of wall thickness, and equal to the intercept for the unbeaten pulp. The pulp was beaten in a Waring blender for 15 min and this was sufficient to remove the S_1 layer as discerned microscopically from the swelling behaviour in a cupriethylene diamine solution. The results are shown in Fig. 4. Birefringence for the beaten fibres is independent of wall thickness, and within experimental error is equal to the intercept for the unbeaten pulp. Thus it is concluded that for this black spruce sample the mean

TABLE 1. *Sources of wood pulp fibres studied*

Species	Source	Pulping Process
Black spruce	33rd, 55th and 80th rings of a 110-year-old tree	60% yield kraft chlorite bleached Holocellulose
Balsam fir	30th and 52nd rings of a 56-year-old tree	Holocellulose
Douglas-fir	146th, 200th, 295th and 372nd rings of a 379-year-old tree	Holocellulose
White pine	33rd and 71st rings of a 73-year-old tree	Holocellulose
Shortleaf pine	20th ring of a 23-year-old tree	Holocellulose
Loblolly pine	12th ring of a 62-year-old tree	60% yield kraft chlorite bleached

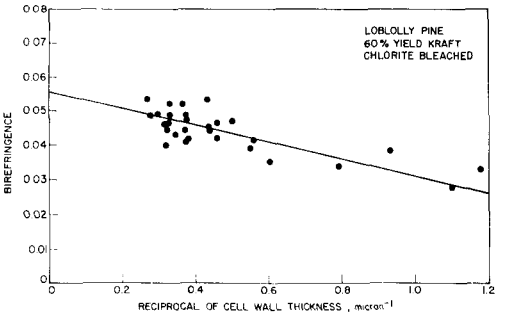

FIG. 10. Plot of birefringence against reciprocal of cell-wall thickness for loblolly pine, 60% yield kraft, chlorite bleached.

thickness of the S_1 layer is independent of the total thickness of the cell wall, as in case II.

Douglas-fir, balsam fir, black spruce holocellulose

Data for samples of these species are given in Figs. 5, 6, and 7. They all show the same linear relationship established above. From the regression line, two quantities of interest can be derived. The intercept on the ordinate gives directly the birefringence of the delignified cell-wall material. The slope of the line gives the combined thickness of the S_1 and S_3 layers. These quantities together with their limits of error are shown in Table 2.

The magnitude of the birefringence of the cell wall has special significance for it can yield information on the degree of orientation of its chemical components. This aspect will be discussed in detail in a subsequent paper. The close similarity of the intercept on the ordinate for the three species suggests that Douglas-fir and balsam fir also obey the relationship of case II, with the S_1 and S_3 layer thicknesses being independent of the S_2 layer thickness.

The combined thicknesses of the S_1 and S_3 layers differ significantly between species with an average around 0.21μm. Although no attempt has been made to confirm this value independently, it is in good agreement with published data, obtained from electron microscopy of sections. The S_1 layer is given by Meier (1955) as 0.20μm and by Jayme and Fengel (1962) as between 0.12 and 0.35μm; the S_3 layer is given as 0.07–0.08μm by Jayme and Fengel (1962) and 0.10–0.15μm by Liese (1960).

White pine and shortleaf pine holocellulose

The behaviour described earlier is not followed for all species. Figure 8 shows that for white pine no correlation exists between birefringence and the reciprocal of cell-wall thickness.

Thus this species obeys the equation derived for case I, for which the thickness of the S_1 and S_3 layers increases proportionately with the total thickness of the cell wall. The sparse data of shortleaf pine given in Fig. 9 show a similar pattern.

If it is assumed that the value of birefringence of the pulped cell wall is 0.056, the combined S_1 and S_3 layers are for white pine 0.38μm (or 18% of the total wall thickness) and for shortleaf pine 0.9μm (or 20% of the total wall thickness). No independent data are available for

TABLE 2. *Birefringence and $S_1 + S_3$ layer thicknesses for Douglas-fir, balsam fir, and black spruce*

Species	Birefringence of the cell-wall material	95% confidence limits of birefringence		$S_1 + S_3$ layer thickness (micrometer)	95% confidence limits of $S_1 + S_3$ thickness (micrometer)	
		From	To		From	To
Douglas-fir	0.0553	0.0523	0.0583	0.249	0.169	0.328
Balsam fir	0.0560	0.0532	0.0588	0.169	0.103	0.236
Black spruce	0.0565	0.0555	0.0575	0.206	0.188	0.225

white pine, but the very high value for shortleaf pine is consistent with published work on a similar species, longleaf pine, which indicates that the S_1 and S_3 layers are unusually thick. The electron micrographs of latewood fibres published by Mark (1967) and Dunning (1969) show S_1 and S_3 layers that are each of the order of 0.5–1.0μm thick.

Loblolly pine, 60% yield kraft, chlorite bleached

Not all pines follow the pattern of the previous section. The data of loblolly pine (Fig. 10) fall on a line of significant slope, similar to the data of spruce and Douglas-fir and balsam fir.

CONCLUSION

The birefringence of holocellulose fibres is controlled by the relative thicknesses of the S_1, S_2, and S_3 layers. For four softwoods, the S_1 and S_3 layers although variable from fibre to fibre, are independent of the total wall thickness, whereas for two species, white pine and shortleaf pine, their thickness increases with total wall thickness. Measurement of birefringence permits a precise determination of the average combined thicknesses of these layers, and the results are in good agreement with previous data.

REFERENCES

DUNNING, C. E. 1969. The structure of longleaf-pine latewood. II. Intertracheid membranes and pit membranes. Tappi 52(7): 1335.

HSU, H-Y., M. RICHARTZ, AND Y-K. LIANG. 1947. A generalized intensity formula for a system of retardation plates. J. Opt. Soc. Am. 37:99.

JAYME, G., AND D. FENGEL. 1962. Elektronenoptische Beobachtungen über den Feinbau von Nadelholzzellen. Papier, Darmstadt. 16(10a):519.

KERR, T., AND I. W. BAILEY. 1934. The cambium and its derivative tissues. No. X. Structure, optical properties and chemical composition of the so-called middle lamella. J. Arnold Arboretum 15:327.

LIESE, W. 1960. The structure of the tertiary wall in tracheids and wood fibres. Holz Roh-Werkst. 18:296.

MARK, R. E. 1967. Cell-wall mechanics of tracheids. Yale University Press.

MEIER, H. 1955. Über den Zellwandabbau durch Holzvermorschungspilze und die submikroskopiche struktur von Fichtentracheiden und Birkenholzfasern. Holz Roh- Werkst. 13: 323.

PAGE, D. H. 1969. A method for determining the fibrillar angle in wood tracheids. J. Roy. Microscop. Soc. 90(2):137.